



Insight Into the Molecular Dynamic Simulation Studies of Reactive Oxygen Species in Native Skin Membrane

Dharmendra K. Yadav^{1,2*†}, Surendra Kumar^{1,2†}, Eun-Ha Choi³, Praveen Sharma⁴, Sanjeev Misra³ and Mi-Hyun Kim^{1,2*}

¹ College of Pharmacy, Gachon University of Medicine and Science, Incheon, South Korea, ² Gachon Institute of Pharmaceutical Science & Department of Pharmacy, College of Pharmacy, Gachon University, Incheon, South Korea, ³ Plasma Bioscience Research Center/PDP Research Center, Kwangwoon University, Seoul, South Korea, ⁴ Department of Biochemistry, All India Institute of Medical Sciences, Jodhpur, India

OPEN ACCESS

Edited by:

Andres Trostchansky,
Facultad de Medicina, Universidad
de la República, Uruguay

Reviewed by:

Rajeev K. Singla,
Netaji Subhas Institute of Technology,
India

Debasish Bandyopadhyay,
The University of Texas Rio Grande
Valley, United States

Rohit Gundamaraju,
University of Tasmania, Australia

*Correspondence:

Dharmendra K. Yadav
dharmendra30oct@gmail.com
Mi-Hyun Kim
kmh0515@gachon.ac.kr

[†] These authors have contributed
equally to this work.

Specialty section:

This article was submitted to
Experimental Pharmacology
and Drug Discovery,
a section of the journal
Frontiers in Pharmacology

Received: 26 April 2018

Accepted: 30 May 2018

Published: 27 June 2018

Citation:

Yadav DK, Kumar S, Choi E-H,
Sharma P, Misra S and Kim M-H
(2018) Insight Into the Molecular
Dynamic Simulation Studies
of Reactive Oxygen Species in Native
Skin Membrane.
Front. Pharmacol. 9:644.
doi: 10.3389/fphar.2018.00644

In recent years, the role of reactive oxygen species (ROS) in regulating cancer cell apoptosis, inflammation, cell ischemia, and cell signaling pathways has been well established. The most common sources of intracellular ROS are the mitochondrial electron transport system, NADH oxidase, and cytochrome P450. In this study, we investigated the dynamics and permeability of ROS using molecular dynamics (MD) simulations on native skin-lipid bilayer membranes. Native skin-lipid bilayers are composed of ceramide, cholesterol, and free fatty acid in an almost equal molar ratio (1:1:1). Dynamic distribution studies on ROS, i.e., hydrogen peroxide (H₂O₂) and O₂ (¹O₂ by analogy), revealed that these species interact with cholesterol as a primary target in lipid peroxidation of the skin-lipid bilayer. Moreover, the permeability of ROS, i.e., H₂O₂, hydroxyl radicals (HO), hydroperoxy radical (HOO), and O₂, along the skin-lipid bilayer was measured using free energy profiles (FEPs). The FEPs showed that in spite of high-energy barriers, ROS traveled through the membrane easily. Breaching the free energy barriers, these ROS permeated into the membrane, inflicting oxidative stress, and causing apoptosis. Collectively, the insight acquired from simulations may result in a better understanding of oxidative stress at the atomic level.

Keywords: molecular dynamics simulation, reactive oxygen species, free energy profile, lipid peroxidation, oxidative stress

INTRODUCTION

The stratum corneum, the outermost layer of the skin, is the primary barrier to many harmful molecules including reactive oxygen species (ROS) that penetrate the skin (Elias, 1983). Over the last few decades, the role of ROS has been documented in the process of aging and in several chronic diseases such as atherosclerosis, diabetes, Alzheimer's disease, asthma, rheumatoid arthritis, and neurodegenerative diseases (Lacy et al., 1998; Bauerova and Bezek, 1999; Droge, 2002; Bahorun et al., 2006; Ivanova et al., 2013). ROS have also been implicated in many forms of cancer, such as melanoma (Fridman et al., 2007; Kim et al., 2009; Keidar et al., 2011; Arndt et al., 2013; Ishaq et al., 2014a), cervical (Leduc et al., 2009; Ahn et al., 2011), lung (Kim et al., 2011), breast (Kim et al., 2010; Wang et al., 2013), glioblastoma (Vandamme et al., 2012; Kaushik et al., 2013), and

ovarian cancer (Iseki et al., 2012; Utsumi et al., 2013). ROS, i.e., superoxide ($O_2^{\cdot-}$) and hydroperoxy radical (HOO) are produced through the mitochondrial electron transport chain within cells. To address the toxicity of ROS, the host defense mechanism produces superoxide dismutase that converts $O_2^{\cdot-}$ into less reactive hydrogen peroxide (H_2O_2). However, in the presence of trace metals, H_2O_2 generates distinctly toxic hydroxyl radicals (HO) via fenton-type reactions (Cheng and Li, 2007; Prousek, 2007). Additionally, singlet oxygen, a prominent species in inducing melanoma, is produced via non-enzymatic oxidation of the skin-lipid bilayer at some point in the photosensitization reaction (Foote, 1968; Rawls and Van Santen, 1970). Consequently, these ROS makes the skin membrane vulnerable to peroxidative damage via triggering lipid peroxidation and targeting the sterol component of the skin-lipid bilayer (Logani and Davies, 1980; Girotti, 2008). Oxidized lipids present in the skin membrane have the ability to modify the membrane properties, especially in terms of permeability (Grzełńska et al., 1979; Richter, 1987; Wratten et al., 1992; Chen and Yu, 1994; Tai et al., 2010; Jurkiewicz et al., 2012). Furthermore, the distribution of various types of ROS at the interface between the lipid bilayer and water facilitates the understanding of lipid peroxidation and radical scavenging via membrane antioxidants in an organism (Afri et al., 2002; Gamliel et al., 2008). In recent years, cold atmospheric plasmas (CAPs) have been proven to have great potential in different areas of medical science, including melanoma research. The possible selectivity toward melanoma might be due to the substantial rise in intracellular ROS in response to oxidative stress occurring in membranes of cancer cells compared to that in normal cell membranes upon the same CAP treatment (Ja Kim et al., 2013; Ishaq et al., 2014a,b; Kaushik et al., 2014; Kim and Chung, 2016). However, the underlying mechanisms for the enhanced concentration of ROS in cancer cell membranes remain elusive (Van der Paal et al., 2016). Another explanation could be the increased expression of aquaporins (AQPs), a membrane protein family that facilitates the diffusion of water across cellular membranes, in melanoma/non-melanoma cells (Verkman et al., 2008; Ramadan et al., 2017). It is shown that various cancer cell lines have expressed elevated levels of certain AQPs (Shi et al., 2012; Papadopoulos and Saadoun, 2015; Yan et al., 2015, 2017). Moreover, because of the similarity between ROS (i.e., H_2O_2 , HOO, HO, O_2) and water (Bienert et al., 2006; Bienert and Chaumont, 2014), AQPs are able to facilitate the passive diffusion of these ROS through membranes, which leads to increased oxidative stress.

The skin-lipid bilayer membrane is the outermost cellular organ that acts as a barrier and controls the transportation of materials. Several experimental studies on phospholipid vesicles as simple models for cell membranes have been accomplished to infer the oxidation of lipids, structural and chemical modifications, and transportation of ROS through the phospholipid membranes (Hammer et al., 2013; Hong et al., 2014; Tero et al., 2014; Szili et al., 2015; Ki et al., 2016; Maheux et al., 2016). In addition, once the lipids are oxidized, they accumulate within the bilayer and further

contribute to changes in structural organization and packing of membrane lipid components. Consequently, those structural changes abate the mechanical strength, permeability, and fluidity of the lipid bilayer membrane (Beranova et al., 2010; Jarerattanachat et al., 2013; Van der Paal et al., 2016).

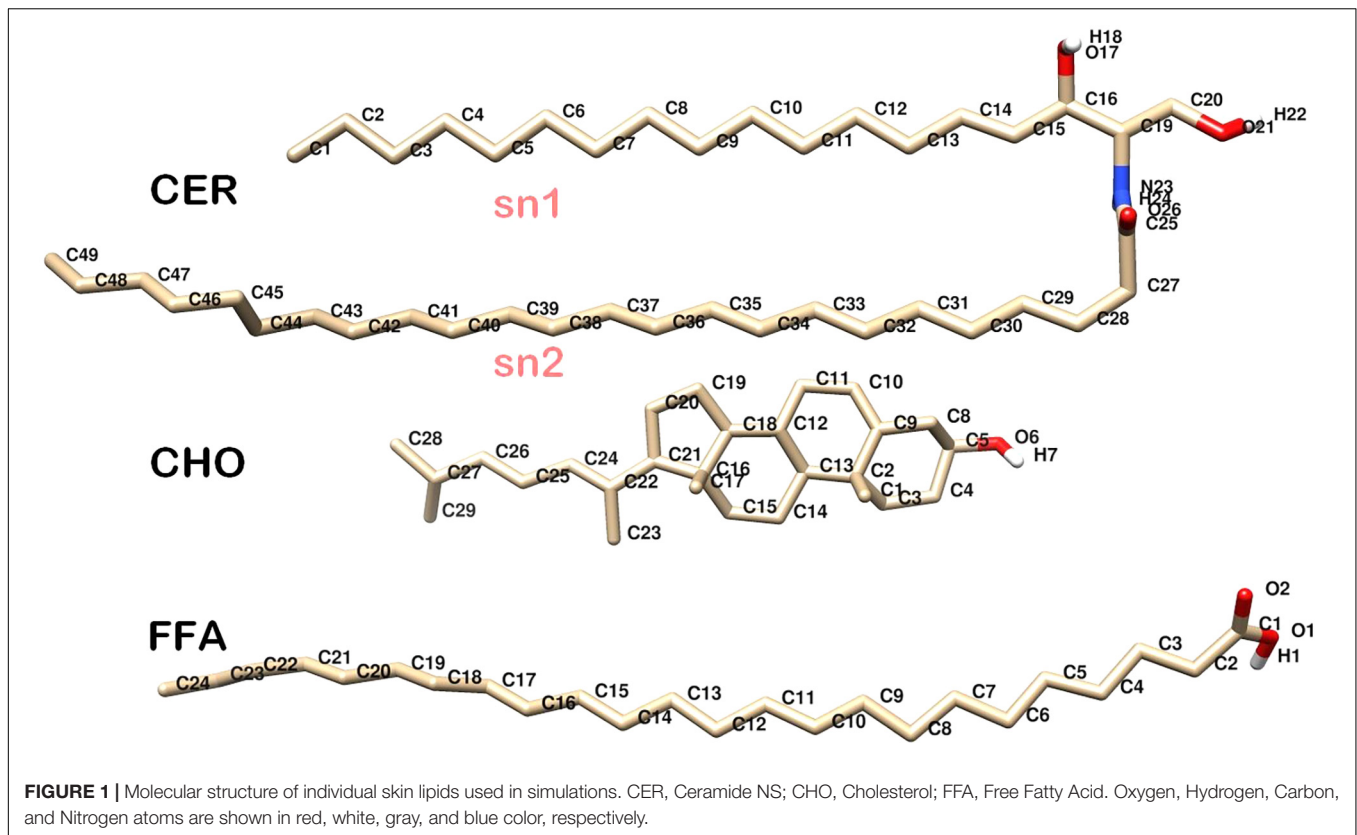
The present work describes how the native skin-lipid bilayer was constructed and simulated. Subsequently, we performed the dynamics and distribution of ROS (especially H_2O_2 and O_2) at the interface between the skin-lipid bilayer and water, and throughout the lipid bilayer. Since H_2O_2 is the primary species that undergoes fenton-type reaction to generate various radicals and O_2 , as an analogy of 1O_2 , has a prime role in lipid oxidation, particularly in the sterol component of the skin-lipid bilayer (Engelmann et al., 2007; Cordeiro et al., 2012). Thus, we further investigated the interaction of ROS (H_2O_2 and O_2) with hydrophilic headgroups of the skin-lipid bilayer. Furthermore, the permeability of different ROS, i.e., H_2O_2 , HO, HOO, and O_2 (1O_2 by analogy), through the skin-lipid bilayer membrane was evaluated using the umbrella sampling (US) method by calculating the potential mean of forces (PMFs) (Roux, 1995; Van Der Spoel et al., 2005). Since these ROS have different tendencies for permeation, thus from the PMFs, the free energy barriers for permeation across the lipid bilayer may be derived. The sampling of the entire system can be advantageous in the US method as compared to the traditional molecular dynamics (MD) simulation. Indeed, Cordeiro (2014) used the US method to calculate the FEPs of various ROS in POPC (1-palmitoyl-2-oleoyl-sn-glycero-3-phosphocholine) membranes and observed at par with experimental outcomes. Similarly, Gajula et al. (2017) carried out multi-scale simulation studies on the permeation of various solutes through the skin-lipid bilayer membrane. The present study extends the US method to study the permeation of ROS through the skin-lipid bilayer membrane.

MATERIALS AND METHODS

Computational Scheme

The structures of the individual components of native skin-lipid bilayer used in this study, which are ceramide (CER), cholesterol (CHO), and free fatty acid (FFA), are shown in **Figure 1**. The skin-lipid bilayer was constructed using the PACKMOL package (Martinez et al., 2009). The native skin-lipid bilayer includes 52 CER, 50 CHO, and 52 FFA at an almost equal molar ratio (1:1:1) and 5120 water molecules. The force field parameters for CER, CHO and FFA were based on prior studies (Berger et al., 1997; Hölftje et al., 2001) and proved to be steady with experimental results. The CH_2 and CH_3 groups of CER were represented by united carbon atoms with zero partial charge, and the polar hydrogen atoms were included explicitly (Das et al., 2009). The simple point charge model was used for the water molecules (Berendsen et al., 1981). The ROS parameters were taken from a study reported by Cordeiro (2014; Supplementary Table S1).

All simulations were performed in the constant-temperature, constant-pressure ensemble (NPT) using the GROMACS 5.1.4



MD package (Berendsen et al., 1995; Van Der Spoel et al., 2005; Hess et al., 2008; Pronk et al., 2013). The temperature was controlled at 310.15 K by a Nose–Hoover thermostat with a time constant of 0.5 ps and coupled separately to lipid or water molecules. Pressure was controlled at 1 bar using a Parrinello–Rahman barostat with a time constant of 5 ps and compressibility of 4.5×10^{-5} bar with semi-isotropic coupling. A time step of 2fs was used for all simulations. The cut-off distances for coulombic interactions and van der Waals interactions were both set at 1.2 nm. The system was periodic in all Cartesian directions.

The built skin-lipid bilayer was first energy-minimized using the steepest descent algorithm, followed by constant-temperature, constant-volume ensemble (NVT) equilibration for 2 ns under restrained conditions. The equilibrated bilayer was further simulated for 10 ns under NPT ensemble before the structure was submitted to simulate annealing, where the system was heated upto 360 K and cooled to 310.15 K in a systematic manner to obtain well-hydrated lipid bilayer heads. The system was further equilibrated for 50 ns, followed by 200 ns of production simulation under NPT ensemble conditions. The size of the obtained bilayer was 5.02 nm \times 5.02 nm \times 11.3 nm. The final structure of the native skin-lipid bilayer structure (**Figure 2**) was used to study the membrane properties, i.e., area per lipid (APL), bilayer thickness, and tail order parameters. Furthermore, the modeled native skin-lipid bilayer structure was used to study the ROS distribution at the interface between the lipid membrane

and water, as well as to estimate the free energy profiles (FEFs).

Analysis of Native Skin-Lipid Bilayer Membrane Properties

The membrane properties, i.e., APL, bilayer thickness, and tail order parameters, of CER and FFA were measured from the simulated native skin-lipid bilayer membrane. The APL describes the packing of a lipid bilayer. To calculate APL, the box-x vector of the lipid bilayer was defined along with estimates of error on last 50 ns of the simulation. Similarly, the membrane thickness, an important parameter in describing the properties of the system, was calculated using the APLVORO software (Lukat et al., 2013) on last 50 ns of the simulation trajectory. In this analysis, the headgroups of each lipid component (i.e., atoms O21 for CER, O6 for CHO, and O₂ for FFA) were used as the key atoms, and membrane thickness was defined as the average position between the headgroups of both leaflets. Finally, the ordering or alignment of the lipid hydrocarbon tails of CER and FFA could be determined by defining the tail order parameters (S_z) per carbon atom C_n , as follows:

$$S_z = \frac{3}{2} \langle \cos^2(\theta_z) \rangle - \frac{1}{2}$$

where θ_z is the angle between the vector from C_{n-1} to C_{n+1} and the bilayer normal (z -axis). Here $S_z = 1$ represents perfect alignment of the tails with the z -axis, $S_z = 0$ represents random

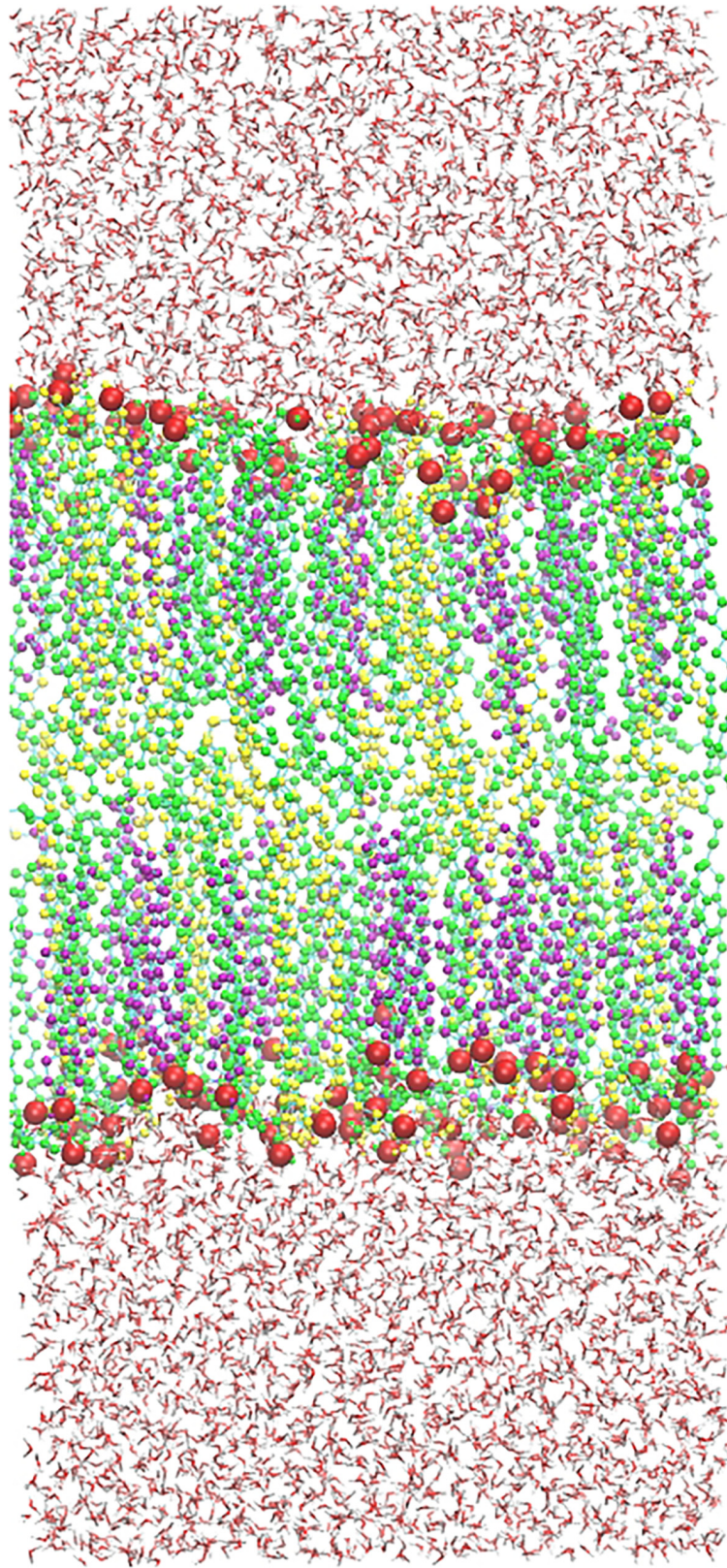


FIGURE 2 | Native structure of a skin lipid bilayer containing 52 CER (Green), 50 CHO (Purple), 52 FFA (Yellow) molecules, and 5210 water molecules. Polar heads (Oxygen) are shown in red sphere [van der Waals (VDW)].

orientation, and $S_z = -0.5$ represents perpendicular alignment to the bilayer normal (Gupta and Rai, 2015; Piggot et al., 2017).

Simulations of ROS (H_2O_2 and O_2) Distribution and Dynamics

Hydrogen peroxide is a primary ROS that is produced by mitochondria in events mediated by external stimuli (i.e., exposure of cells to UV or other oxidative stress conditions). It plays a role in apoptotic signaling via cell-to-cell transmission (Rojkind et al., 2002; Pletjushkina et al., 2006). In the event of fenton-type reaction, H_2O_2 generates toxic radicals, i.e., HO (Prousek, 2007). In addition, singlet oxygen ($^1\text{O}_2$) species play an important role in lipid oxidation via photosensitization reactions, targeting the sterol component of the lipid bilayer and similarly disrupting the integrity and fluidity of the lipid bilayer. Thus, in order to comprehend the interactions and distributions of ROS, especially H_2O_2 (as a primary species) and O_2 ($^1\text{O}_2$ by analogy), the lower (25 molecules) and higher (50 molecules) concentrations of each ROS were placed separately over lipid bilayer head in two pre-equilibrated system. The concentrations selected corresponds to those found in mitochondria (experimentally measured molar fraction of ca. 0.5%) (Cadenas and Davies, 2000). After 20 ns of restrained equilibration under NPT ensemble, each system was simulated for 30 ns at 310.15 K and 1 bar pressure. The density profile along the z -direction and the distance between the ROS (H_2O_2 and O_2) and the upper headgroups of the skin-lipid bilayer membrane were evaluated.

Permeation Free Energy Profiles

The FEPs of each ROS molecule throughout the skin-lipid bilayer was calculated by the US methodology. The US methodology makes use of additional energy terms, known as bias, in the system to ensure efficient sampling throughout the reaction coordinate. The US method has already been described in the literature (Gupta et al., 2016; Gajula et al., 2017; Van der Paal et al., 2017), however, in brief, for sampling the entire phase of the skin-lipid bilayer membrane. Starting from the upper water leaflet, crossing the lipid bilayer structure, and ending in the lower water leaflet, multiple ROS molecules were placed in the native skin membrane system at different xy - and z -planes. The reaction coordinate of the system was chosen in the z -dimension, where $z = 0$ corresponds to the center of mass (COM) of lipid molecules (CER + CHO + FFA). To save computational resources, eight umbrella windows were sampled during each simulation, keeping a distance of 1.2 nm (12 Å) among consecutive windows, starting at ~ 4.8 nm from the COM of the bilayer as shown in **Figure 3**. For each ROS, multiple systems were created. Each system was energy-minimized and equilibrated under NPT ensemble, while keeping the ROS molecules fixed at the current position. Each US simulation lasted for 20 ns, and last 10 ns were used for analysis, i.e., to acquire the US histograms and to calculate the FEPs. In each US simulation, the ROS molecules were free to move in the xy -plane, but their movement in the z -direction was constrained by applying a harmonic bias with a spring

constant of $2000 \text{ kJ}\cdot\text{mol}^{-1}\cdot\text{nm}^{-2}$. FEPs are constructed via the weighted histogram analysis method (WHAM), as implemented in GROMACS (Hub et al., 2010). To improve the statistical accuracy of sampling, the final energy profiles were obtained by averaging six FEPs for each ROS.

RESULTS AND DISCUSSION

Calculation of Native Skin-Lipid Bilayer Membrane Properties

The APL of native skin-lipid bilayer is shown in Supplementary Figure S1. The calculated APL was $0.32 \pm 0.003 \text{ nm}$, which was comparable to that reported in previous studies (0.31 nm) (Gupta and Rai, 2015) and ($0.33 \pm 0.01 \text{ nm}$) (Wang and Klauda, 2018). Similarly, the thickness of the native skin-lipid bilayer membrane was calculated on the last 50 ns of simulation and was found to be 4.98 nm, which was comparable to those reported in previous experiments (5.12 nm) (Gupta and Rai, 2015) and (5.17 nm) (Das et al., 2009).

Likewise, the tail order parameters were calculated for the hydrophobic chains of CER and FFA, and are shown in Supplementary Figure S2. The order parameters of CER for sn1 and sn2 are low near C16 and C24, respectively, and increased as we moved toward the mid-bilayer and decreased further down toward the center of the bilayer. Moreover, in the presence of CER and CHOL, the order parameters for FFA chain length followed the similar trend as that for the CER chain. Similar chain lengths of CER and FFA led to proper inter-digitization and ordering of tails.

Distribution and Dynamics of ROS at the Membrane and Water Interface

To understand the arrangement of the different components in each system under investigation, the density profiles of the individual lipid components and ROS along the z -direction were plotted, which are shown in **Figure 4**.

The density distribution for the individual lipid components and H_2O_2 species (H_2O_2 -25: 25 molecules of H_2O_2 , H_2O_2 -50: 50 molecules of H_2O_2) were qualitatively similar (**Figures 4A,B**). The density profile of CER showed high density near the headgroups region, low density at the bilayer center, and almost constant density between these two bilayer regions, which was due to the ordered tail atoms. The density profile of FFA is similar to that of CER, except that high density was observed at the bilayer center. Moreover, the density profile of CHO showed two shoulders at $z = \sim 1.5 \text{ nm}$ and low density at the bilayer center, suggesting that because of the shorter chain length of CHO, they mostly resided at the interface between the lipid membrane and water, and the alkyl tails were aligned with the alkyl chains of CER. Furthermore, because of the shorter chain length of CHO, the bilayer center consists primarily of CER and FFA tails and they overlapped with each other. The distribution of H_2O_2 was mostly at the interface between the lipid membrane and water, and no H_2O_2 molecule was found inside the bilayer center (Supplementary Figure S3).

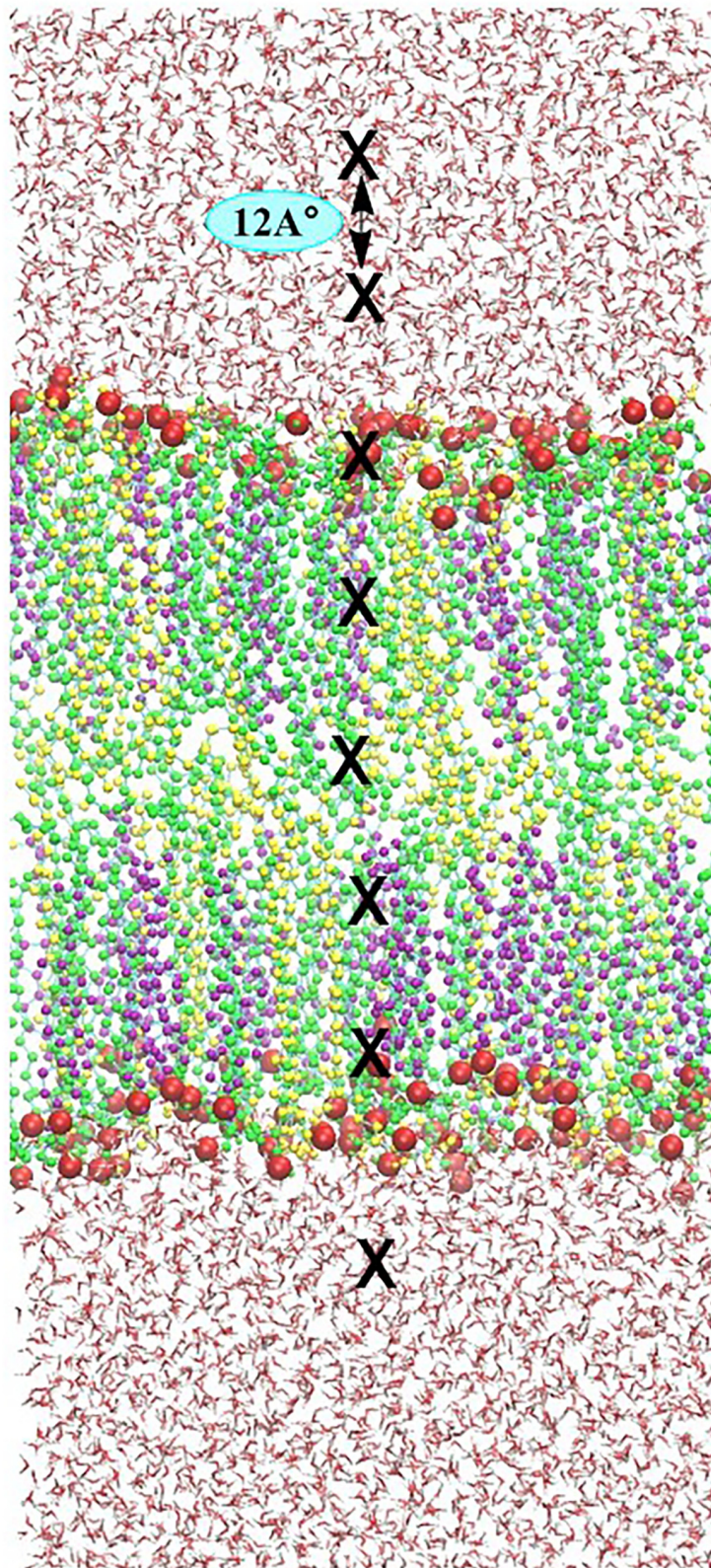
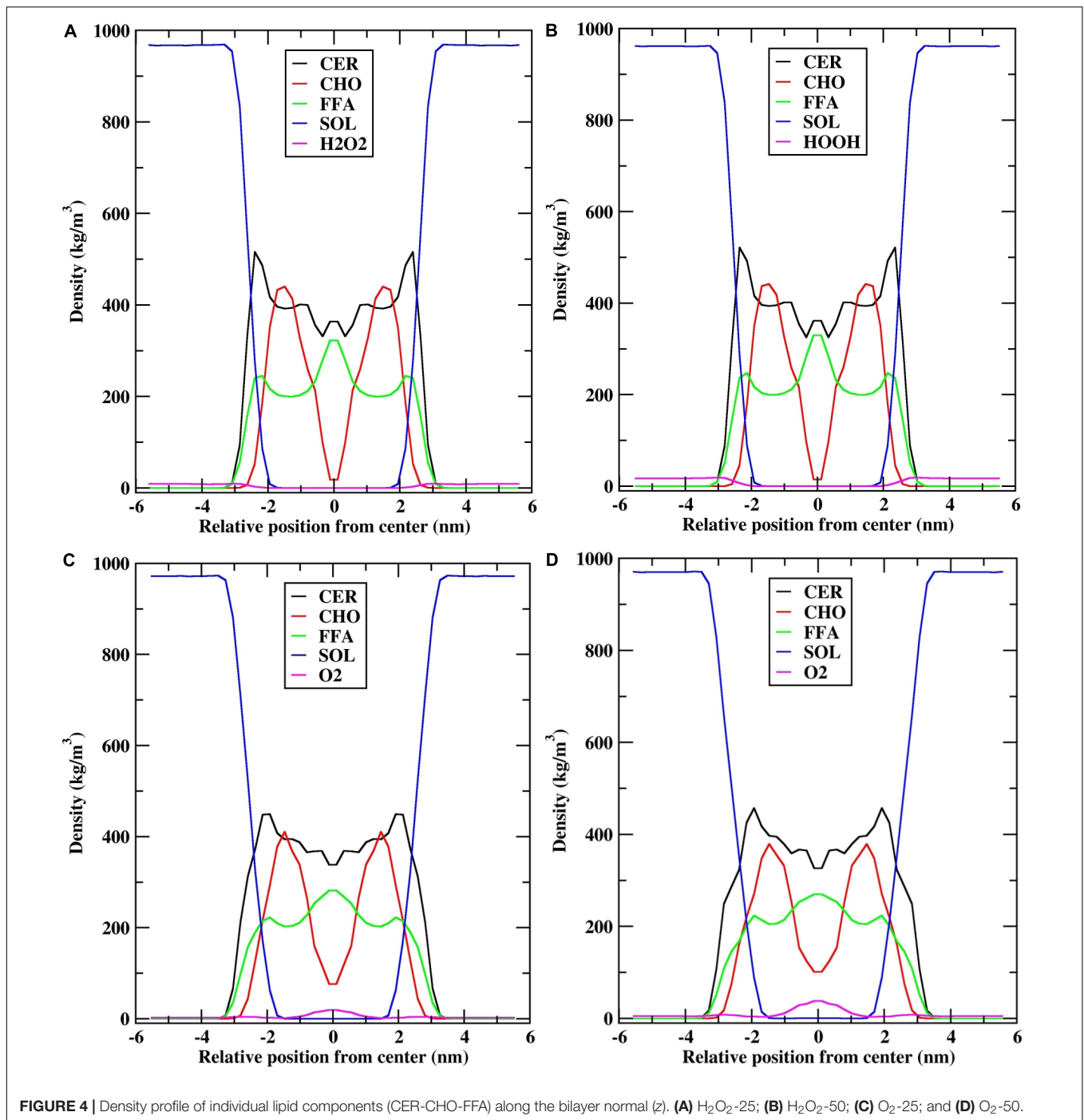


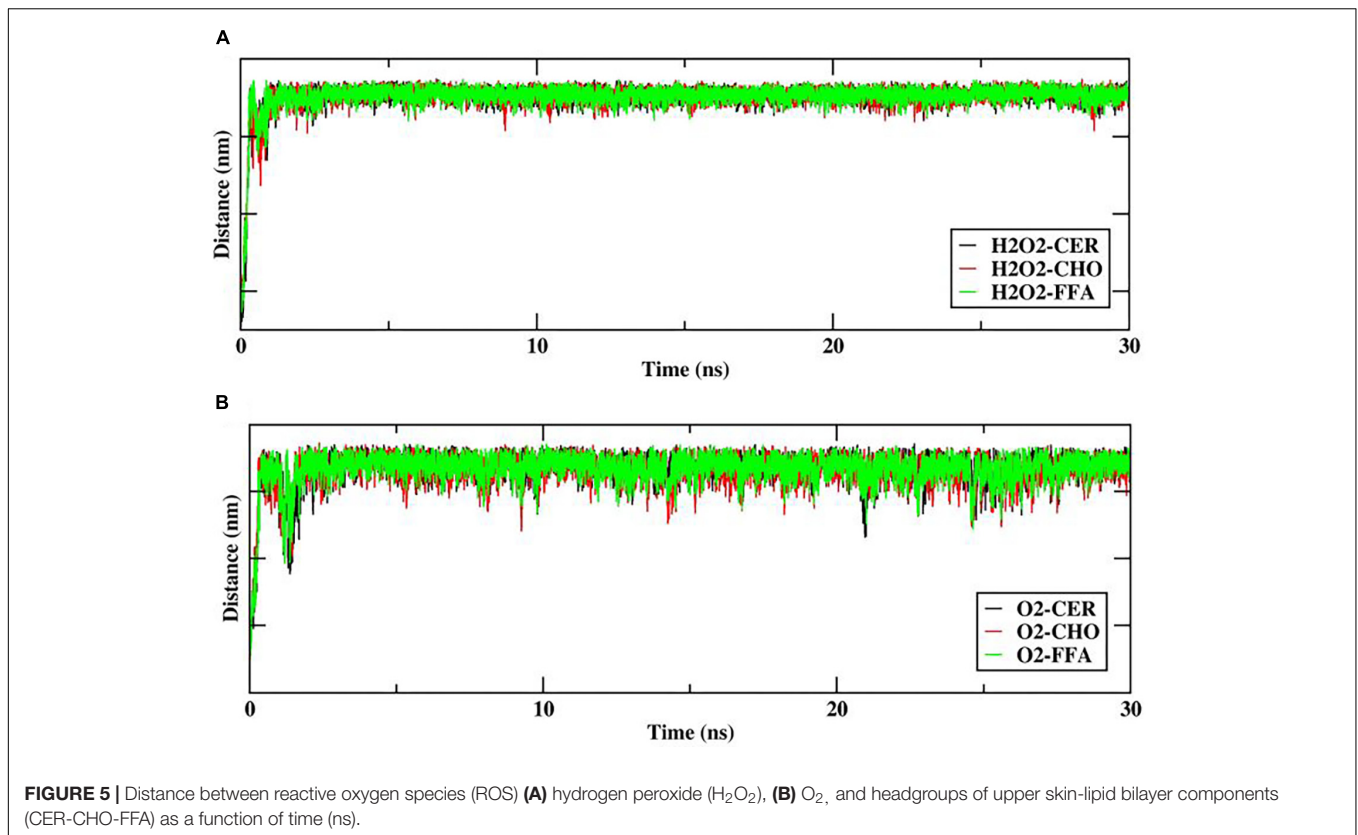
FIGURE 3 | Illustration of the umbrella sampling (US) simulation set-up. Eight umbrella windows separated by 12 Å (position of ROS depicted by block crosses) are sampled in one simulation. In consecutive simulations, each species is shifted by 0.12 Å. To sample the entire membrane system, 33 simulations are performed, yielding a total of 264 umbrella histograms from which a potential mean of forces (PMF) is constructed.



Likewise, the density distributions of O_2 -25 (25 molecules of O_2) and O_2 -50 (50 molecules of O_2) were qualitatively similar to each other. However, they were different from the density profiles of H_2O_2 (Figures 4C,D). During the simulation, the distribution of the O_2 species affected the density profile of all lipid components. CER had a shoulder in the headgroups region, while the height of the shoulder decreased. The densities of CHO and FFA at the bilayer center decreased, corresponding to the fact that the bilayer center was occupied by O_2 molecules

(Supplementary Figure S4). In addition, the density of O_2 was higher at the bilayer center in O_2 -50, whereas it was slightly lower in O_2 -25, suggesting that as the number of O_2 molecules increased, they penetrated deeper into the bilayer and occupied the space between the two leaflets. However, the lipid bilayer membrane preserved its symmetry with little perturbation.

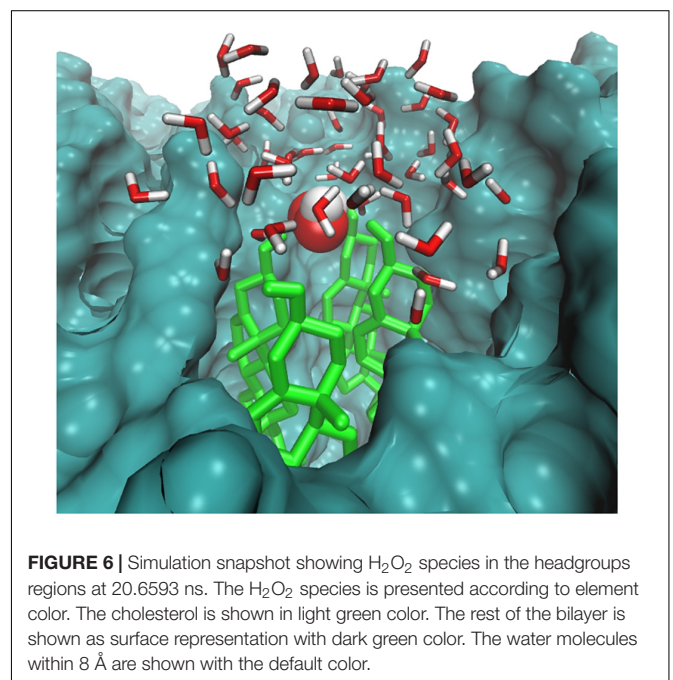
In order to explore the interactions/contacts of H_2O_2 and O_2 species with the lipid bilayer membrane components, the



distances between the H_2O_2 or O_2 species and the headgroups of the upper lipid bilayer were measured and are shown in **Figure 5**.

The distance between H_2O_2 and the headgroups of the upper lipid bilayer is shown in **Figure 5A**. Furthermore, H_2O_2 as primary species may generate various species that mainly targets hydrophilic or double-bond containing lipid components. Thus as the simulation progressed, all H_2O_2 species made multiple contacts with the headgroup of the lipid component. **Figure 5A** clearly shows that among all of the headgroups, H_2O_2 made multiple contacts with the headgroups of CHO. Moreover, selected snapshots showed the interaction profile between H_2O_2 and CHO, in which H_2O_2 was surrounded by the headgroups of CHO molecules (**Figure 6** and Supplementary Figure S3), revealing that in *in situ* fenton-type reactions, H_2O_2 may generate other species that structurally modify CHO to cause perturbational changes in the skin-lipid bilayer structure that may result in oxidative stress.

Likewise, Cordeiro (2014) simulated the O_2 species in POPC lipid bilayers and stated that O_2 prefers to reside within the interior membrane. Since the role of singlet oxygen in sterol peroxidation has already been established (Kulig and Smith, 1973), we further investigated its role in interactions with native skin-lipid bilayers. The distance between the O_2 species and the headgroups of upper lipid bilayers was measured, which is shown in **Figure 5B**. During simulation, the O_2 species made maximum multiple contacts with the headgroups of CHO in the upper skin-lipid bilayer. To show the interaction profile



between O_2 and the CHO headgroups, a snapshot was selected as a representative (**Figure 7** and Supplementary Figure S4). The interaction profile and final simulated structure revealed that besides preferring to reside in the interior of the bilayer,

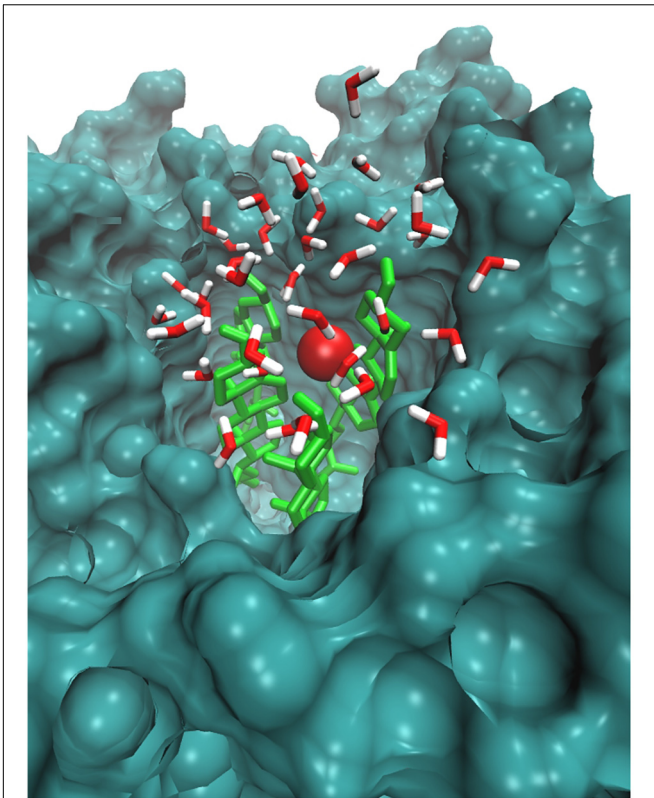


FIGURE 7 | Simulation snapshot showing O_2 species in the headgroups regions at 25.4265 ns. The O_2 species is presented according to element color. The cholesterol is shown in light green color. The rest of the bilayer is shown as surface representation with dark green color. The water molecules within 8 Å are shown with the default color.

some O_2 species also engaged with the CHO headgroups. The final simulated structure showed that during simulation, O_2 traveled from the upper aqueous layer through the lipid bilayer

TABLE 1 | Transfer free energies (ΔG) of all investigated reactive oxygen species (ROS) in a native skin-lipid bilayer (CER-CHO-FFA) membrane.

ROS	ΔG (kJ.mol ⁻¹)
H_2O_2	37.61 ± 1.92
HOO	25.03 ± 1.75
HO	24.06 ± 1.07
O_2	-4.70 ± 0.57

toward the bilayer center. This was supported by comparing the distance between H_2O_2 or O_2 and the headgroups of the upper skin-lipid bilayer, and a maximum distance for O_2 as compared to H_2O_2 was observed. These findings supported the fact that while traveling alongside the skin-lipid bilayer, O_2 might have had access to potential peroxidation sites (cholesterol is more prone to undergo peroxidation that can result in perturbational changes in the membrane (Neto and Cordeiro, 2016).

Effect of ROS on Skin-Lipid Bilayer Membrane Permeability

To better explain and understand the permeability of various ROS through the skin-lipid bilayer membrane, averaged PMF profiles were measured for all ROS and are shown in **Figure 8**. The bootstrapping standard deviations from PMF profiles are shown in Supplementary Figure S5. In **Figure 8**, the membrane shown on the background depicts the location of different regions of the bilayer structure, and the transfer free energy barriers associated with these profiles are compiled in **Table 1**. In **Figure 8**, H_2O_2 , HO, and hydroperoxyl radical (HOO) displayed energy minima before entering the lipid bilayer near the headgroups region (~ -2.9 nm), which corresponded to interactions with the headgroups of the lipid bilayer. However, because of the additional oxygen atom, the HOO species displayed greater interaction compared to HO. Meanwhile, the O_2 species showed a slight increase in free energy (~ 0.25 kJ/mol) near the headgroup

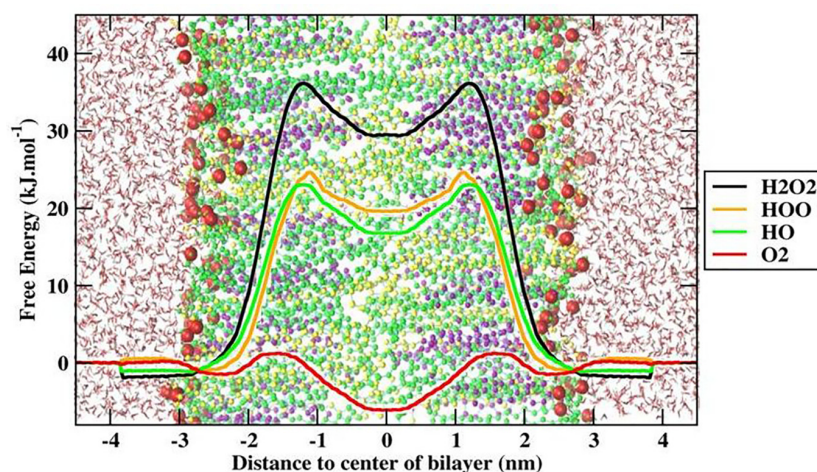


FIGURE 8 | Free energy profile (FEP) of different ROS across skin-lipid bilayer (CER-CHO-FFA) membrane.

region. These observations are consistent with those presented in a previous study by Gupta et al. (2016), where the free energy of hydrophilic species slightly decreased but that of hydrophobic species slightly increased. Moving toward the bilayer center, the role of lipid bilayer membrane as a permeation barrier can be explained from the drastic increase in free energy with all ROS species except for O_2 . The transfer free energy increased and reached a maximum in the hydrophobic core of H_2O_2 (~37.61 kJ/mol), HOO (~25.04 kJ/mol), and HO (~24.06 kJ/mol), and then decreased to ~30.51, ~20.20, and ~16.62 kJ/mol, respectively, at the bilayer center. However, because of the hydrophobic nature of the O_2 species, its PMF profile was entirely different from those of other types of ROS. The transfer free energy after crossing the headgroup region of the lipid bilayer decreased to ~-1.32 kJ/mol and then increased to ~2.66 kJ/mol. This new energy barrier at ~1.5 nm for O_2 can be assigned to the bulky ring of cholesterol in the skin-lipid bilayer. The transfer free energy further decreased (~-6.1 kJ/mol) and displayed an energy-minimum at the bilayer center because of the depletion of lipids in the center and contributed to the accumulation of O_2 species at the center of the skin-lipid bilayer (Subczynski and Hyde, 1983). Comparing the free energy barriers of all ROS, the permeation of H_2O_2 was most hindered with an activation free energy estimated to be 37.61 ± 1.92 kJ/mol, which is comparatively higher than other computational (33 ± 4 kJ/mol) (Cordeiro, 2014) and experimental (36.8 kJ/mol) (Mathai and Sitaramam, 1994) findings. Such differences in transfer free energy may be due to the high ordering of CER and FFA chains and the existence of the native skin-lipid bilayer in the gel phase (Paloncova et al., 2014; Gupta and Rai, 2015). The free energy barriers for HO and HOO are highly similar and there is almost no significant barrier for O_2 , which is in agreement with the preceding experimental study and corresponds to the permeability of different types of ROS (Simon et al., 2008). All PMF profiles showed local energy minima in the center of the bilayer that correspond to regions with decreased lipid bilayer density. **Figure 4** displays the density profile of the lipid components, and the decrease in the density of cholesterol in the center of the bilayer can be attributed to the smaller structure of cholesterol. Moreover, the notably higher free energy barriers for H_2O_2 , HO, and HOO can be explained from the observation that these species established multiple hydrogen bonding with the surrounding water molecules, and as soon as they lose their hydration water before penetrates into the lipid membrane. In fact, Cordeiro (2014) showed that H_2O_2 can build up twice the number of H-bonds (4.5) compared with HO (2) and HOO (2.3).

CONCLUSION

Hydrogen peroxide is the primary ROS produced in mitochondria in events caused by oxidative stress. H_2O_2 further undergoes fenton-type reactions *in situ* to generate various radicals/species. Along with these species, singlet oxygen (1O_2) has been shown to hamper the fluidity and integrity

of skin-lipid bilayer membranes by peroxidizing sterol, one of the key components of skin-lipid bilayer membranes. The present study investigated the interaction of H_2O_2 and O_2 (1O_2 by analogy) with the headgroups of skin-lipid bilayer membranes and estimated the permeability of various types of ROS, i.e., H_2O_2 , HO, HOO, and O_2 , across the skin-lipid bilayer membrane. The results obtained in the present study illustrated that H_2O_2 and O_2 make multiple contacts with the headgroups of the skin-lipid bilayer membrane, and among the different headgroups, cholesterol has maximum contact with these species. The study also showed that besides residing on the interface between the skin-lipid bilayer and water, O_2 also prefers to concentrate more in the center of the skin-lipid bilayer by traveling along the lipid tail of the skin-lipid bilayer membrane. Thus, whilst O_2 travels along the lipid bilayer, it might have gained access to potential peroxidation sites of the lipid components. The major components of skin-lipid bilayers are ceramide, cholesterol, and free fatty acid, and peroxidation studies have already proven that cholesterol is more prone to peroxidation *in situ*. Thus, the present study supported the experimental evidence. We also determined the permeability of various types of ROS across the skin-lipid bilayer membrane. The FEPs in terms of PMFs indicated that in spite of the high free energy barrier, ROS (i.e., H_2O_2 , HO, and HOO) in the native skin-lipid bilayer membrane easily travel across the membrane. The minimal free energy barrier of O_2 suggests that these species do not have any barrier. Thus, they are easily transported along the skin-lipid bilayer, and reside in the bilayer center. By breaching the free energy barriers, all ROS would be able to permeate the membrane, causing oxidative stress that might lead to apoptosis. All of the results were obtained for the native skin-lipid bilayer membrane (equimolar ratio of lipid components). However, further investigation will be performed with varying concentrations of cholesterol, as it is the primary target for lipid peroxidation. Collectively, the insights obtained from simulations might help in gaining a better understanding of oxidative stress at the atomic level.

AUTHOR CONTRIBUTIONS

DY conceived and designed the project and collected data from the literature and databases. SK and DY performed the experiments, analyzed the data, and wrote the manuscript. M-HK, E-HC, PS, and SM provided the molecular modeling lab facility. All authors contributed to the interpretation and discussion of the results and read and approved the final version of the manuscript.

FUNDING

This study was supported by the Basic Science Research Program of the National Research Foundation of Korea (NRF) funded by the Ministry of Education, Science and Technology (Nos. 2017R1C1B2003380 and 2017R1E1A1A01076642) and the Science and Engineering Research Board, New Delhi for financial support through the Young Scientist Project

SB/YS/LS-130/2014 at the All India Institute of Medical Sciences (AIIMS), Jodhpur, India. The National Institute of Supercomputing and Network/Korea Institute of Science and Technology Information provided supercomputing resources including technical support (No. KSC-2017-C1-0013).

REFERENCES

- Afri, M., Gottlieb, H. E., and Frimer, A. A. (2002). Superoxide organic chemistry within the liposomal bilayer; part II: a correlation between location and chemistry. *Free Radic. Biol. Med.* 32, 605–618. doi: 10.1016/S0891-5849(02)00753-0
- Ahn, H. J., Kim, K. I., Kim, G., Moon, E., Yang, S. S., and Lee, J. S. (2011). Atmospheric-pressure plasma jet induces apoptosis involving mitochondria via generation of free radicals. *PLoS One* 6:e28154. doi: 10.1371/journal.pone.0028154
- Arndt, S., Wacker, E., Li, Y. F., Shimizu, T., Thomas, H. M., Morfill, G. E., et al. (2013). Cold atmospheric plasma, a new strategy to induce senescence in melanoma cells. *Exp. Dermatol.* 22, 284–289. doi: 10.1111/exd.12127
- Bahorun, T., Soobrattee, M., Luximon-Ramma, V., and Aruoma, O. (2006). Free radicals and antioxidants in cardiovascular health and disease. *Int. J. Med. Update* 1, 25–41. doi: 10.4314/ijmu.v1i2.39839
- Bauerova, K., and Bezek, A. (1999). Role of reactive oxygen and nitrogen species in etiopathogenesis of rheumatoid arthritis. *Gen. Physiol. Biophys.* 18, 15–20.
- Beranova, L., Cwiklik, L., Jurkiewicz, P., Hof, M., and Jungwirth, P. (2010). Oxidation changes physical properties of phospholipid bilayers: fluorescence spectroscopy and molecular simulations. *Langmuir* 26, 6140–6144. doi: 10.1021/la100657a
- Berendsen, H. J., Postma, J. P., van Gunsteren, W. F., and Hermans, J. (1981). Interaction models for water in relation to protein hydration. *Nature* 224, 175–177.
- Berendsen, H. J., van der Spoel, D., and van Drunen, R. (1995). GROMACS: a message-passing parallel molecular dynamics implementation. *Comput. Phys. Commun.* 91, 43–56. doi: 10.1016/0010-4655(95)00042-E
- Berger, O., Edholm, O., and Jähnig, F. (1997). Molecular dynamics simulations of a fluid bilayer of dipalmitoylphosphatidylcholine at full hydration, constant pressure, and constant temperature. *Biophys. J.* 72, 2002–2013. doi: 10.1016/S0006-3495(97)78845-3
- Bienert, G. P., and Chaumont, F. (2014). Aquaporin-facilitated transmembrane diffusion of hydrogen peroxide. *Biochim. Biophys. Acta* 1840, 1596–1604. doi: 10.1016/j.bbagen.2013.09.017
- Bienert, G. P., Schjoerring, J. K., and Jahn, T. P. (2006). Membrane transport of hydrogen peroxide. *Biochim. Biophys. Acta* 1758, 994–1003. doi: 10.1016/j.bbamem.2006.02.015
- Cadenas, E., and Davies, K. J. (2000). Mitochondrial free radical generation, oxidative stress, and aging. *Free Radic. Biol. Med.* 29, 222–230. doi: 10.1016/S0891-5849(00)00317-8
- Chen, J. J., and Yu, B. P. (1994). Alterations in mitochondrial membrane fluidity by lipid peroxidation products. *Free Radic. Biol. Med.* 17, 411–418. doi: 10.1016/0891-5849(94)90167-8
- Cheng, Z., and Li, Y. (2007). What is responsible for the initiating chemistry of iron-mediated lipid peroxidation: an update. *Chem. Rev.* 107, 748–766. doi: 10.1021/cr040077w
- Cordeiro, R. M. (2014). Reactive oxygen species at phospholipid bilayers: distribution, mobility and permeation. *Biochim. Biophys. Acta* 1838, 438–444. doi: 10.1016/j.bbamem.2013.09.016
- Cordeiro, R. M., Miotto, R., and Baptista, M. S. (2012). Photodynamic efficiency of cationic meso-porphyrins at lipid bilayers: insights from molecular dynamics simulations. *J. Phys. Chem. B* 116, 14618–14627. doi: 10.1021/jp308179h
- Das, C., Noro, M. G., and Olmsted, P. D. (2009). Simulation studies of stratum corneum lipid mixtures. *Biophys. J.* 97, 1941–1951. doi: 10.1016/j.bpj.2009.06.054
- Droge, W. (2002). Free radicals in the physiological control of cell function. *Physiol. Rev.* 82, 47–95. doi: 10.1152/physrev.00018.2001
- Elias, P. M. (1983). Epidermal lipids, barrier function, and desquamation. *J. Invest. Dermatol.* 80, 44s–49s. doi: 10.1111/1523-1747.ep12537108
- Engelmann, F. M., Mayer, I., Gabrielli, D. S., Toma, H. E., Kowaltowski, A. J., Araki, K., et al. (2007). Interaction of cationic meso-porphyrins with liposomes, mitochondria and erythrocytes. *J. Bioenerg. Biomembr.* 39, 175–185. doi: 10.1007/s10863-007-9075-0
- Footo, C. S. (1968). Photosensitized oxygenations and the role of singlet oxygen. *Acc. Chem. Res.* 1, 104–110. doi: 10.1021/ar50004a002
- Fridman, G., Shereshevsky, A., Jost, M. M., Brooks, A. D., Fridman, A., Gutsol, A., et al. (2007). Floating electrode dielectric barrier discharge plasma in air promoting apoptotic behavior in melanoma skin cancer cell lines. *Plasma Chem. Plasma Process.* 27, 163–176. doi: 10.1007/s11090-007-9048-4
- Gajula, K., Gupta, R., Sridhar, D., and Rai, B. (2017). In-Silico skin model: a multiscale simulation study of drug transport. *J. Chem. Inf. Model.* 57, 2027–2034. doi: 10.1021/acs.jcim.7b00224
- Gamliel, A., Afri, M., and Frimer, A. A. (2008). Determining radical penetration of lipid bilayers with new lipophilic spin traps. *Free Radic. Biol. Med.* 44, 1394–1405. doi: 10.1016/j.freeradbiomed.2007.12.028
- Girotti, A. W. (2008). Translocation as a means of disseminating lipid hydroperoxide-induced oxidative damage and effector action. *Free Radic. Biol. Med.* 44, 956–968. doi: 10.1016/j.freeradbiomed.2007.12.004
- Grzelińska, E., Bartosz, G., Gwoździński, K., and Leyko, W. (1979). A spin-label study of the effect of gamma radiation on erythrocyte membrane. Influence of lipid peroxidation on membrane structure. *Int. J. Radiat. Biol. Relat. Stud. Phys. Chem. Med.* 36, 325–334. doi: 10.1080/09553007914551111
- Gupta, R., and Rai, B. (2015). Molecular dynamics simulation study of skin lipids: effects of the molar ratio of individual components over a wide temperature range. *J. Phys. Chem. B* 119, 11643–11655. doi: 10.1021/acs.jpcc.5b02093
- Gupta, R., Sridhar, D. B., and Rai, B. (2016). Molecular dynamics simulation study of permeation of molecules through skin lipid bilayer. *J. Phys. Chem. B* 120, 8987–8996. doi: 10.1021/acs.jpcc.6b05451
- Hammer, M. U., Forbrig, E., Kupsch, S., Weltmann, K.-D., and Reuter, S. (2013). Influence of plasma treatment on the structure and function of lipids. *Plasma Med.* 3, 97–114. doi: 10.1615/PlasmaMed.2014009708
- Hess, B., Kutzner, C., Van Der Spoel, D., and Lindahl, E. (2008). GROMACS 4: algorithms for highly efficient, load-balanced, and scalable molecular simulation. *J. Chem. Theory Comput.* 4, 435–447. doi: 10.1021/ct700301q
- Höltje, M., Förster, T., Brandt, B., Engels, T., von Rybinski, W., and Höltje, H.-D. (2001). Molecular dynamics simulations of stratum corneum lipid models: fatty acids and cholesterol. *Biochim. Biophys. Acta* 1511, 156–167. doi: 10.1016/S0005-2736(01)00270-X
- Hong, S.-H., Szili, E. J., Jenkins, A. T. A., and Short, R. D. (2014). Ionized gas (plasma) delivery of reactive oxygen species (ROS) into artificial cells. *J. Phys. D* 47:362001. doi: 10.1088/0022-3727/47/36/362001
- Hub, J. S., De Groot, B. L., and Van Der Spoel, D. (2010). g_wham - A free weighted histogram analysis implementation including robust error and autocorrelation estimates. *J. Chem. Theory Comput.* 6, 3713–3720. doi: 10.1021/ct100494z
- Iseki, S., Nakamura, K., Hayashi, M., Tanaka, H., Kondo, H., Kajiyama, H., et al. (2012). Selective killing of ovarian cancer cells through induction of apoptosis by nonequilibrium atmospheric pressure plasma. *Appl. Phys. Lett.* 100:113702. doi: 10.1063/1.3694928
- Ishaq, M., Evans, M. D., and Ostrikov, K. K. (2014a). Atmospheric pressure gas plasma-induced colorectal cancer cell death is mediated by Nox2–ASK1 apoptosis pathways and oxidative stress is mitigated by Srx–Nrf2 anti-oxidant system. *Biochim. Biophys. Acta* 1843, 2827–2837. doi: 10.1016/j.bbamcr.2014.08.011
- Ishaq, M., Kumar, S., Varinli, H., Han, Z. J., Rider, A. E., Evans, M. D., et al. (2014b). Atmospheric gas plasma-induced ROS production activates TNF-ASK1 pathway for the induction of melanoma cancer cell apoptosis. *Mol. Biol. Cell* 25, 1523–1531. doi: 10.1091/mbc.e13-10-0590

SUPPLEMENTARY MATERIAL

The Supplementary Material for this article can be found online at: <https://www.frontiersin.org/articles/10.3389/fphar.2018.00644/full#supplementary-material>

- Ivanova, D., Bakalova, R., Lazarova, D., Gadjeva, V., and Zhelev, Z. (2013). The impact of reactive oxygen species on anticancer therapeutic strategies. *Adv. Clin. Exp. Med.* 22, 899–908.
- Ja Kim, S., Min Joh, H., and Chung, T. (2013). Production of intracellular reactive oxygen species and change of cell viability induced by atmospheric pressure plasma in normal and cancer cells. *Appl. Phys. Lett.* 103:153705. doi: 10.1063/1.4824986
- Jarerattanachai, V., Karttunen, M., and Wong-ekkabut, J. (2013). Molecular dynamics study of oxidized lipid bilayers in NaCl solution. *J. Phys. Chem. B* 117, 8490–8501. doi: 10.1021/jp4040612
- Jurkiewicz, P., Olzyska, A., Cwiklik, L., Conte, E., Jungwirth, P., Megli, F. M., et al. (2012). Biophysics of lipid bilayers containing oxidatively modified phospholipids: insights from fluorescence and EPR experiments and from MD simulations. *Biochim. Biophys. Acta* 1818, 2388–2402. doi: 10.1016/j.bbame.2012.05.020
- Kaushik, N. K., Attri, P., Kaushik, N., and Choi, E. H. (2013). A preliminary study of the effect of DBD plasma and osmolytes on T98G brain cancer and HEK non-malignant cells. *Molecules* 18, 4917–4928. doi: 10.3390/molecules18054917
- Kaushik, N. K., Kaushik, N., Park, D., and Choi, E. H. (2014). Altered antioxidant system stimulates dielectric barrier discharge plasma-induced cell death for solid tumor cell treatment. *PLoS One* 9:e103349. doi: 10.1371/journal.pone.0103349
- Keidar, M., Walk, R., Shashurin, A., Srinivasan, P., Sandler, A., Dasgupta, S., et al. (2011). Cold plasma selectivity and the possibility of a paradigm shift in cancer therapy. *Br. J. Cancer* 105, 1295–1301. doi: 10.1038/bjc.2011.386
- Ki, S., Park, J., Sung, C., Lee, C., Uhm, H., Choi, E., et al. (2016). Artificial vesicles as an animal cell model for the study of biological application of non-thermal plasma. *J. Phys. D* 49:085401. doi: 10.1088/0022-3727/49/8/085401
- Kim, G.-C., Lee, H. J., and Shon, C.-H. (2009). The effects of a micro plasma on melanoma (G361) cancer cells. *J. Korean Phys. Soc.* 54, 628–632. doi: 10.3938/jkps.54.628
- Kim, J. Y., Ballato, J., Foy, P., Hawkins, T., Wei, Y., Li, J., et al. (2011). Apoptosis of lung carcinoma cells induced by a flexible optical fiber-based cold microplasma. *Biosens. Bioelectron.* 28, 333–338. doi: 10.1016/j.bios.2011.07.039
- Kim, S. J., and Chung, T. (2016). Cold atmospheric plasma jet-generated RONS and their selective effects on normal and carcinoma cells. *Sci. Rep.* 6:20332. doi: 10.1038/srep20332
- Kim, S. J., Chung, T., Bae, S., and Leem, S. (2010). Induction of apoptosis in human breast cancer cells by a pulsed atmospheric pressure plasma jet. *Appl. Phys. Lett.* 97:023702. doi: 10.1063/1.3462293
- Kulig, M. J., and Smith, L. L. (1973). Sterol metabolism. XXV. Cholesterol oxidation by singlet molecular oxygen. *J. Org. Chem.* 38, 3639–3642. doi: 10.1021/jo00960a050
- Lacy, F., Sheeter, L., Lumicao, M., Wang, B., Sah, R., and Schmid-Schonbein, G. W. (1998). Reactive oxygen species in rheumatoid arthritis. *FASEB J.* 12:A8.
- Leduc, M., Guay, D., Leask, R., and Coulombe, S. (2009). Cell permeabilization using a non-thermal plasma. *New J. Phys.* 11:115021. doi: 10.1088/1367-2630/11/11/115021
- Logani, M., and Davies, R. (1980). Lipid oxidation: biologic effects and antioxidants—a review. *Lipids* 15, 485–495. doi: 10.1007/BF02534079
- Lukat, G., Kruger, J., and Sommer, B. (2013). APL@Voro: a Voronoi-based membrane analysis tool for GROMACS trajectories. *J. Chem. Inf. Model.* 53, 2908–2925. doi: 10.1021/ci400172g
- Maheux, S., Frache, G., Thomann, J., Clément, F., Penny, C., Belmonte, T., et al. (2016). Small unilamellar liposomes as a membrane model for cell inactivation by cold atmospheric plasma treatment. *J. Phys. D* 49:344001. doi: 10.1088/0022-3727/49/34/344001
- Martinez, L., Andrade, R., Birgin, E. G., and Martinez, J. M. (2009). PACKMOL: a package for building initial configurations for molecular dynamics simulations. *J. Comput. Chem.* 30, 2157–2164. doi: 10.1002/jcc.21224
- Mathai, J. C., and Sitaramam, V. (1994). Stretch sensitivity of transmembrane mobility of hydrogen peroxide through voids in the bilayer. Role of cardiolipin. *J. Biol. Chem.* 269, 17784–17793.
- Neto, A. J., and Cordeiro, R. M. (2016). Molecular simulations of the effects of phospholipid and cholesterol peroxidation on lipid membrane properties. *Biochim. Biophys. Acta* 1858, 2191–2198. doi: 10.1016/j.bbame.2016.06.018
- Palconyova, M., DeVane, R. H., Murch, B. P., Berka, K., and Otyepka, M. (2014). Rationalization of reduced penetration of drugs through ceramide gel phase membrane. *Langmuir* 30, 13942–13948. doi: 10.1021/la503289v
- Papadopoulos, M. C., and Saadoun, S. (2015). Key roles of aquaporins in tumor biology. *Biochim. Biophys. Acta* 1848, 2576–2583. doi: 10.1016/j.bbame.2014.09.001
- Piggot, T. J., Allison, J. R., Sessions, R. B., and Essex, J. W. (2017). On the calculation of Acyl chain order parameters from lipid simulations. *J. Chem. Theory Comput.* 13, 5683–5696. doi: 10.1021/acs.jctc.7b00643
- Pletjushkina, O. Y., Fetisova, E., Lyamzaev, K., Ivanova, O. Y., Domnina, L., Vyssokikh, M. Y., et al. (2006). Hydrogen peroxide produced inside mitochondria takes part in cell-to-cell transmission of apoptotic signal. *Biochemistry* 71, 60–67. doi: 10.1134/S0006297906010093
- Pronk, S., Páll, S., Schulz, R., Larsson, P., Bjelkmar, P., Apostolov, R., et al. (2013). GROMACS 4.5: a high-throughput and highly parallel open source molecular simulation toolkit. *Bioinformatics* 29, 845–854. doi: 10.1093/bioinformatics/btt055
- Prousek, J. (2007). Fenton chemistry in biology and medicine. *Pure Appl. Chem.* 79, 2325–2338. doi: 10.1351/pac200779122325
- Ramadan, W. M., Gheida, S. F., El-Ashmawy, A. A., and Shareef, M. M. (2017). Aquaporin-3 expression in common hyperproliferative skin disorders: an immunohistochemical study. *J. Egypt. Women Dermatol. Soc.* 14, 128–136. doi: 10.1097/01.ewx.0000513084.47849.72
- Rawls, H. R., and Van Santen, P. (1970). A possible role for singlet oxygen in the initiation of fatty acid autoxidation. *J. Am. Oil Chem. Soc.* 47, 121–125. doi: 10.1007/BF02640400
- Richter, C. (1987). Biophysical consequences of lipid peroxidation in membranes. *Chem. Phys. Lipids* 44, 175–189. doi: 10.1016/0009-3084(87)90049-1
- Rojkind, M., Dominguez-Rosales, J.-A., Nieto, N., and Greenwel, P. (2002). Role of hydrogen peroxide and oxidative stress in healing responses. *Cell. Mol. Life Sci.* 59, 1872–1891. doi: 10.1007/PL00012511
- Roux, B. (1995). The calculation of the potential of mean force using computer simulations. *Comput. Phys. Commun.* 91, 275–282. doi: 10.1016/0010-4655(95)00053-1
- Shi, Z., Zhang, T., Luo, L., Zhao, H., Cheng, J., Xiang, J., et al. (2012). Aquaporins in human breast cancer: identification and involvement in carcinogenesis of breast cancer. *J. Surg. Oncol.* 106, 267–272. doi: 10.1002/jso.22155
- Simon, S. A., Benos, D. J., and Matalon, S. (2008). *Free Radical Effects on Membranes*. Cambridge, MA: Academic Press.
- Subczynski, W. K., and Hyde, J. S. (1983). Concentration of oxygen in lipid bilayers using a spin-label method. *Biophys. J.* 41, 283–286. doi: 10.1016/S0006-3495(83)84439-7
- Szili, E. J., Hong, S. H., and Short, R. D. (2015). On the effect of serum on the transport of reactive oxygen species across phospholipid membranes. *Biointerphases* 10:029511. doi: 10.1116/1.4918765
- Tai, W.-Y., Yang, Y.-C., Lin, H.-J., Huang, C.-P., Cheng, Y.-L., Chen, M.-F., et al. (2010). Interplay between structure and fluidity of model lipid membranes under oxidative attack. *J. Phys. Chem. B* 114, 15642–15649. doi: 10.1021/jp1014719
- Tero, R., Suda, Y., Kato, R., Tanoue, H., and Takikawa, H. (2014). Plasma irradiation of artificial cell membrane system at solid–liquid interface. *Appl. Phys. Express* 7:077001. doi: 10.7567/APEX.7.077001
- Utsumi, F., Kajiyama, H., Nakamura, K., Tanaka, H., Mizuno, M., Ishikawa, K., et al. (2013). Effect of indirect nonequilibrium atmospheric pressure plasma on anti-proliferative activity against chronic chemo-resistant ovarian cancer cells *in vitro* and *in vivo*. *PLoS One* 8:e81576. doi: 10.1371/journal.pone.0081576
- Van der Paal, J., Neyts, E. C., Verlackt, C. C., and Bogaerts, A. (2016). Effect of lipid peroxidation on membrane permeability of cancer and normal cells subjected to oxidative stress. *Chem. Sci.* 7, 489–498. doi: 10.1039/C5SC02311D
- Van der Paal, J., Verheyen, C., Neyts, E. C., and Bogaerts, A. (2017). Hampering Effect of cholesterol on the permeation of reactive oxygen species through phospholipids bilayer: possible explanation for plasma cancer selectivity. *Sci. Rep.* 7:39526. doi: 10.1038/srep39526
- Van der Spoel, D., Lindahl, E., Hess, B., Groenhof, G., Mark, A. E., and Berendsen, H. J. (2005). GROMACS: fast, flexible, and free. *J. Comput. Chem.* 26, 1701–1718. doi: 10.1002/jcc.20291

- Vandamme, M., Robert, E., Lerondel, S., Sarron, V., Ries, D., Dozias, S., et al. (2012). ROS implication in a new antitumor strategy based on non-thermal plasma. *Int. J. Cancer* 130, 2185–2194. doi: 10.1002/ijc.26252
- Verkman, A. S., Hara-Chikuma, M., and Papadopoulos, M. C. (2008). Aquaporins—new players in cancer biology. *J. Mol. Med.* 86, 523–529. doi: 10.1007/s00109-008-0303-9
- Wang, E., and Klauda, J. B. (2018). Simulations of pure ceramide and ternary lipid mixtures as simple interior stratum corneum models. *J. Phys. Chem. B* 122, 2757–2768. doi: 10.1021/acs.jpcc.8b00348
- Wang, M., Holmes, B., Cheng, X., Zhu, W., Keidar, M., and Zhang, L. G. (2013). Cold atmospheric plasma for selectively ablating metastatic breast cancer cells. *PLoS One* 8:e73741. doi: 10.1371/journal.pone.0073741
- Wratten, M. L., van Ginkel, G., van't Veld, A. A., Bekker, A., van Faassen, E. E., and Sevanian, A. (1992). Structural and dynamic effects of oxidatively modified phospholipids in unsaturated lipid membranes. *Biochemistry* 31, 10901–10907. doi: 10.1021/bi00159a034
- Yan, D., Talbot, A., Nourmohammadi, N., Sherman, J. H., Cheng, X., and Keidar, M. (2015). Toward understanding the selective anticancer capacity of cold atmospheric plasma—a model based on aquaporins (Review). *Biointerphases* 10:040801. doi: 10.1116/1.4938020
- Yan, D., Xiao, H., Zhu, W., Nourmohammadi, N., Zhang, L. G., Bian, K., et al. (2017). The role of aquaporins in the anti-glioblastoma capacity of the cold plasma-stimulated medium. *J. Phys. D* 50:055401. doi: 10.1088/1361-6463/aa53d6

Conflict of Interest Statement: The authors declare that the research was conducted in the absence of any commercial or financial relationships that could be construed as a potential conflict of interest.

Copyright © 2018 Yadav, Kumar, Choi, Sharma, Misra and Kim. This is an open-access article distributed under the terms of the Creative Commons Attribution License (CC BY). The use, distribution or reproduction in other forums is permitted, provided the original author(s) and the copyright owner are credited and that the original publication in this journal is cited, in accordance with accepted academic practice. No use, distribution or reproduction is permitted which does not comply with these terms.